

---

---

*Chapter 5*  
*Experimental – Carvedilol*  
*loaded Alginate Microspheres*

---

---

## **5.1 MATERIALS AND METHODS**

### **5.1.1 Materials**

- Carvedilol was a gift sample from Torrent Research Centre, Ahmedabad, India.
- Sodium alginate, n-octanol, calcium chloride, Span 80<sup>®</sup> were procured from S. D. Fine Chemicals, Mumbai, India.
- Potassium phosphate monobasic (KH<sub>2</sub>PO<sub>4</sub>), Sodium hydroxide, Methanol and Hydrochloric acid were procured from SD Fine chemicals, Mumbai, India.
- A dialysis membrane (cut-off Mw 12000) was procured from Hi Media, India.
- All other chemicals and reagents used in the study were of analytical grade.

### **5.1.2 Equipments**

- Eurostar high speed stirrer (IKA Labortechnik, Germany)
- Remi high speed magnetic stirrer (Remi, MS500, Remi equipments, Mumbai)
- Malvern particle size analyzer (Malvern Mastersizer 2000, Malvern Instruments, UK)
- UV-VIS spectrophotometer (Shimadzu UV1610, Japan)
- Light transmission microscope (Olympus Optical Co. Ltd., Japan)
- Scanning electron microscopy (JSM 5610 LV, Jeol Datum Ltd., Japan)
- Differential Scanning Calorimeter (Mettler Toledo DSC 822e, Japan)
- X-ray diffractometer (Bruker AXS D8 Advance, with X-ray source of Cu, Wavelength 1.5406 Å and Si(Li) PSD detector)

## **5.2 Preparation of Alginate microspheres**

The emulsification method described by Wan et al. (Wan et al., 1992) was utilized for the preparation of microspheres followed by cross linking with calcium chloride. Carvedilol was dispersed in an aqueous solution containing 3% w/v sodium alginate. The solution was dispersed in n-octanol containing 2% v/v Span 80 using a Eurostar (IKA Labortechnik, Germany) high speed stirrer at 1800 rpm. The ratio of the aqueous to n-octanol phase used was 1:20. The resultant W/O emulsion was stirred for 30 min. Calcium chloride solution (2%) was added drop wise and the dispersion

was stirred for another 5 min. The microspheres were collected by vacuum filtration, washed three times with isopropyl alcohol and dried in air at room temperature. Various variables like drug: polymer ratio, concentration of cross linking agent and time of cross linking were considered in the optimization of the formulation.

### **5.3 Experimental design**

Optimization using factorial designs is a powerful, efficient and systemic tool that shortens the time required for the development of pharmaceutical dosage forms and improves research and development work. Factorial designs, where all the factors are studied in all possible combinations, are considered to be the most efficient in estimating the influence of individual variables and their interactions using minimum experiments (Singh B. et al, 2002). The application of factorial design in pharmaceutical formulation development has played a key role in understanding the relationship between the independent variables and the responses to them (Vandervoort, J, et al, 2000). The independent variables are controllable whereas responses are dependent. The contour plot gives a visual representation of the values of the response. This helps the process of optimization by providing an empirical model equation for the response as a function of the different variables (Martinez-Sancho et al., 2004; Kincl et al., 2005; Mehta, AK. et al, 2007; Dhiman et al., 2008).

Various batches of alginate microspheres were prepared based on the  $2^3$  factorial design. The independent variables were drug : polymer weight ratio ( $X_1$ ), calcium chloride concentration ( $X_2$ ) and cross linking time ( $X_3$ ). The independent variables and their levels are shown in Table 5.1. Particle size of the microspheres ( $Y_1$ ) and *in vitro* mucoadhesion ( $Y_2$ ) were taken as response parameters as the dependent variables. Table 5.2 shows the independent and dependent variables.

**Table 5.1 Factorial design parameters and experimental conditions.**

Factors	Levels used, Actual (coded)	
	Low (-1)	High (+1)
X <sub>1</sub> =Drug: polymer weight ratio	0.5:1	1:1
X <sub>2</sub> =Concentration of CaCl <sub>2</sub> (%)	2	4
X <sub>3</sub> =Cross linking time (min)	5	10

**5.4 Characterization of the microspheres**

Characterization of the alginate microspheres was carried out as per the methods described in **Section 4.5** for following studies:

**5.4.1. Particle size measurements**

**5.4.2. Surface morphology**

**5.4.3 Flow Properties**

**5.4.4 Determination of encapsulation efficiency**

The microspheres (5 mg) loaded with carvedilol were crushed and added in a mixture of 10 ml of phosphate buffer pH 6.2 and methanol (9:1) under stirring. The mixture was filtered and the amount of carvedilol was determined spectrophotometrically at 242 nm on UV spectrophotometer (Shimadzu UV1610, Japan). It was confirmed from preliminary UV studies that the presence of dissolved polymers did not interfere with the absorbance of the drug at 242 nm. The percentage encapsulation efficiency was calculated using equation (5.1).

$$\% \text{ Encapsulation efficiency} = \frac{\text{Actual loading}}{\text{Theoretical loading}} \times 100 \quad \dots\dots\dots 5.1$$

**5.4.5 Measurement of in vitro mucoadhesion**

**5.4.6 Differential scanning calorimetry (DSC) analysis**

**5.4.7 X-ray diffraction (XRD) studies**

#### 5.4.8 In vitro drug release

The drug release profiles of carvedilol loaded alginate microspheres were evaluated using method described in Section 4.5.8.

#### 5.5 Optimization data analysis and model-validation

ANOVA was used to establish the statistical validation of the polynomial equations generated by Design Expert® software (version 7.1.3, Stat-Ease Inc, Minneapolis, MN). Fitting a multiple linear regression model to a 2<sup>3</sup> factorial design gave a predictor equation which was a first-order polynomial, having the form:

$$Y=b_0+b_1X_1+b_2 X_2+b_3 X_3+b_{12} X_1 X_2+b_{13} X_1X_3 +b_{23} X_2X_3+b_{123} X_1X_2X_3 \quad \dots 5.2$$

where Y is the measured response associated with each factor level combination; b<sub>0</sub> is an intercept representing the arithmetic average of all quantitative outcomes of 8 runs; b<sub>1</sub> to b<sub>123</sub> are regression coefficients computed from the observed experimental values of Y; and X<sub>1</sub>, X<sub>2</sub> and X<sub>3</sub> are the coded levels of independent variables. The terms X<sub>1</sub>X<sub>2</sub>, X<sub>2</sub>X<sub>3</sub> and X<sub>1</sub>X<sub>3</sub> represent the interaction terms. The main effects (X<sub>1</sub>, X<sub>2</sub> and X<sub>3</sub>) represent the average result of changing one factor at a time from its low to high value. The interaction terms show how the response changes when two factors are changed simultaneously. The polynomial equation was used to draw conclusions after considering the magnitude of coefficients and the mathematical sign it carries, i.e., positive or negative. A positive sign signifies a synergistic effect, whereas a negative sign stands for an antagonistic effect (Dhiman et al., 2008).

In the model analysis, the responses: the particle size of the microspheres and in vitro mucoadhesion of all model formulations were treated by Design-Expert® software. The best fitting mathematical model was selected based on the comparisons of several statistical parameters including the coefficient of variation (CV), the multiple correlation coefficient (*R*<sup>2</sup>), adjusted multiple correlation coefficient (adjusted *R*<sup>2</sup>), and the predicted residual sum of square (PRESS), proved by Design- Expert® software. Among them, PRESS indicates how well the model fits the data, and for the chosen model it should be small relative to the other models under consideration. Level of significance was considered at P<0.05. Three dimensional response surface

plots and two dimensional contour plots resulting from equations were obtained by the Design Expert<sup>®</sup> software. Subsequently, the desirability approach was used to generate the optimum settings for the formulations (Huang et al., 2005; Narendra et al., 2005)

Linear model:

$$Y = b_1X_1 + b_2X_2 + b_3X_3 \quad \dots\dots\dots 5.3$$

2FI (interaction) model:

$$Y = b_1X_1 + b_2X_2 + b_3X_3 + b_{12}X_1X_2 + b_{13}X_1X_3 + b_{23}X_2X_3 \quad \dots\dots\dots 5.4$$

### **5.6 Histology studies**

The study carried out as per the method described in Section 4.5.11.

### **5.7 Stability study**

Stability studies of alginate microspheres of carvedilol were carried out as per method described in Section 4.5.12.

## **5.8 RESULTS AND DISCUSSION**

### **5.8.1 Particle size**

The size of all the eight batches of microspheres prepared in this study was in the range of 26.36–54.32  $\mu\text{m}$  (Table 5.2), which is favorable for intranasal absorption. Preliminary studies showed that as the concentration of polymer was increased, the particle size also proportionally increased. Low alginate concentrations (1%, w/v and 2%, w/v) resulted in clumping of microspheres, whereas high sodium alginate concentration (4%, w/v) resulted in formation of discrete larger microspheres (90  $\mu\text{m}$ ). This could be attributed to an increase in the relative viscosity at higher concentration of polymer and formation of larger particles during emulsification. Hence, the optimized concentration of 3% w/v was selected for preparing the different batches of the microspheres.

## 5. Experimental - Carvedilol loaded Alginate Microspheres

The size of the microspheres was increased with an increase in drug loading. This can be attributed to the corresponding increase in viscosity of drug-polymer dispersion comprising the internal phase of the emulsion. The viscosity increase within the internal phase results in the generation of a coarser emulsion with larger droplets, leading eventually to the formation of larger microspheres (Bhardwaj et al., 1995). Similar increase in the size of microspheres was also observed with increase in calcium chloride concentration as well as cross-linking time. The addition of higher amount of  $\text{Ca}^{2+}$  will result in relatively more cross-linking of the guluronic acid units of sodium alginate, thereby leading to formation of larger microspheres. Similarly, increasing the cross linking time will increase the extent of cross linking and thereby increase the particle size.

**Table 5.2 Formulation of the microspheres utilizing  $2^3$  factorial design.**

Batch No.	X1	X2	X3	Y1*	Y2*	% Encapsulation Efficiency*
ALCR1	0.5:1	2	5	26.36±1.24	85.28±1.86	56.05±0.98
ALCR2	1:1	2	5	43.28±2.36	76.12±1.29	41.19±1.56
ALCR3	0.5:1	4	5	32.85±1.85	82.26±2.08	51.59±3.14
ALCR4	1:1	4	5	48.94±2.57	74.75±1.82	38.23±2.45
ALCR5	0.5:1	2	10	5.46±1.92	78.65±1.58	52.29±1.38
ALCR6	1:1	2	10	54.32±2.21	72.28±2.45	39.44±2.67
ALCR7	0.5:1	4	10	37.64±2.04	74.24±1.98	50.39±1.59
ALCR8	1:1	4	10	50.58±1.68	69.25±1.56	36.62±1.84

\*Values are expressed as mean ± SD. Y1 and Y2 are particle size and in vitro mucoadhesion respectively.

### 5.8.2 Surface morphology

The microspheres were found to be discrete and spherical in shape and had nearly smooth surface. No difference in the morphology was observed between placebo and

**5. Experimental - Carvedilol loaded Alginate Microspheres**

---

drug-loaded microspheres (Fig. 5.1 and 5.2) suggesting that the drug may be present in the bulk of the microspheres and not surface associated.

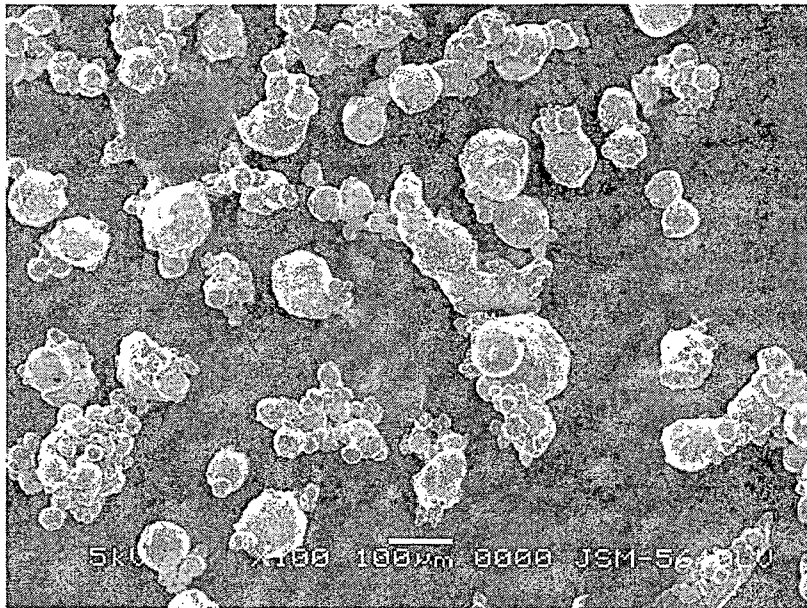


**Fig. 5.1 SEM Photograph of placebo alginate microspheres**

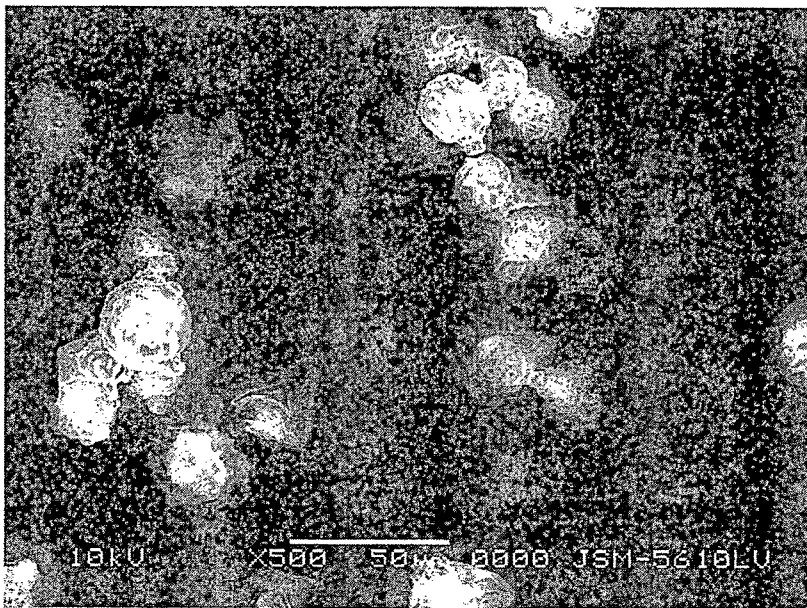


**Fig. 5.2 SEM Photograph of CRV loaded alginate microspheres**

### 5.8.3 Flow Properties

The results of flow properties measurements are shown in Table 5.3. The values of angle of repose were in the range of 26.38<sup>0</sup> to 34.68<sup>0</sup> which is within the normal acceptable range of 20<sup>0</sup> – 40<sup>0</sup> (Wells and Aulton, 1988). The microspheres thus showed reasonably good flow potential. The values of compressibility index were in the range 14.39±2.54 to 19.24±2.21, also indicating good flow characteristics of the microspheres.

**Table 5.3 Flow properties of CRV loaded Alginate microspheres**

Batch No.	Angle of repose( $\theta$ )	Compressibility Index (%)
ALCR1	27.84±2.34	14.39±2.54
ALCR2	32.94±1.96	16.35±1.78
ALCR3	30.62±2.53	17.98±1.82
ALCR4	33.64±1.69	16.22±1.54
ALCR5	28.47±1.65	15.31±1.84
ALCR6	26.38±2.14	16.52±2.41
ALCR7	34.68±2.49	19.24±2.21
ALCR8	31.57±2.56	15.28±2.53

### 5.8.4 Encapsulation efficiency (EE)

The % EE was found to be in the range between 36.62 and 56.18. The % EE showed a dependence on drug loading, amount of cross linking agent and time of cross linking. The formulations loaded with higher amount of drug exhibited higher encapsulation efficiencies (Table 5.2). The encapsulation efficiency, however, showed an inverse relationship with increasing calcium chloride concentration and cross-linking time (Table 5.2). Both these factors lead to an increase in cross link density, which will reduce the free volume spaces within the polymer matrix and hence, a reduction in encapsulation efficiency is observed.

### 5.8.5 In vitro mucoadhesion

The results of in vitro mucoadhesion (Table 5.2) showed that all the batches of microspheres had satisfactory mucoadhesive property ranging from 69.25 to 85.28% (Fig. 5.3) and could adequately adhere to nasal mucosa. The results also showed that with increasing polymer ratio, higher mucoadhesion was observed. This could be attributed to the availability of higher amount of polymer for interaction with mucus. Increase in calcium chloride concentration and cross linking time decreased the mucoadhesive property of the microspheres. Quite a few studies have shown that the prerequisite for good mucoadhesion is the high flexibility of polymer backbone structure and of its polar functional groups. Such a flexibility of the polymer chains, however, is reduced if the polymer molecules are cross linked either with each other or with coagulation agents like calcium ions. Although the cross-linked microspheres will absorb water, they are insoluble and will not form a liquid gel on the nasal epithelium but rather a more solid gel-like structure. This decrease in flexibility imposed upon polymer chains by the cross-linking makes it more difficult for cross-linked polymers to penetrate the mucin network (Peppas and Buri, 1985). Thus, cross linking effectively limits the length of polymer chains that can penetrate the mucus layer and could possibly decrease the mucoadhesion strength of the microspheres (Illum et al., 1987).

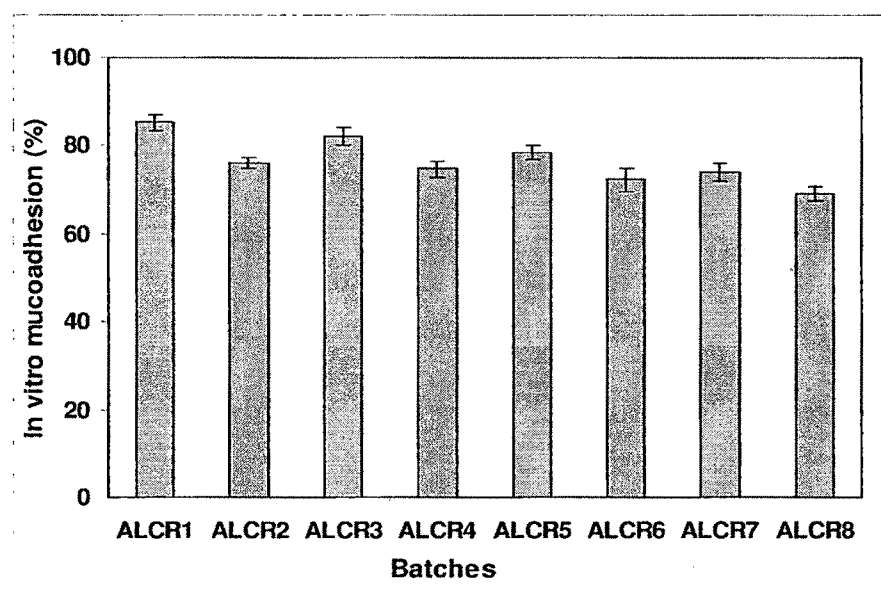


Fig. 5.3 Percentage in vitro mucoadhesion for different batches of microspheres

### 5.8.6 Differential scanning calorimetry (DSC) analysis

DSC is very useful in the investigation of the thermal properties of microspheres, providing both qualitative and quantitative information about the physicochemical state of drug inside the microspheres (Dubernet, 1995). There is no detectable endotherm if the drug is present in a molecular dispersion or solid solution state in the polymeric microspheres loaded with drug (Mu and Feng, 2001). DSC thermograms of pure carvedilol, placebo alginate microspheres and carvedilol loaded alginate microspheres are displayed in Fig. 5.4. Carvedilol shows a sharp peak at 122 °C due to melting, but in case of carvedilol loaded microspheres, no characteristic peak was observed at 122 °C, suggesting that carvedilol is molecularly dispersed in the matrix.

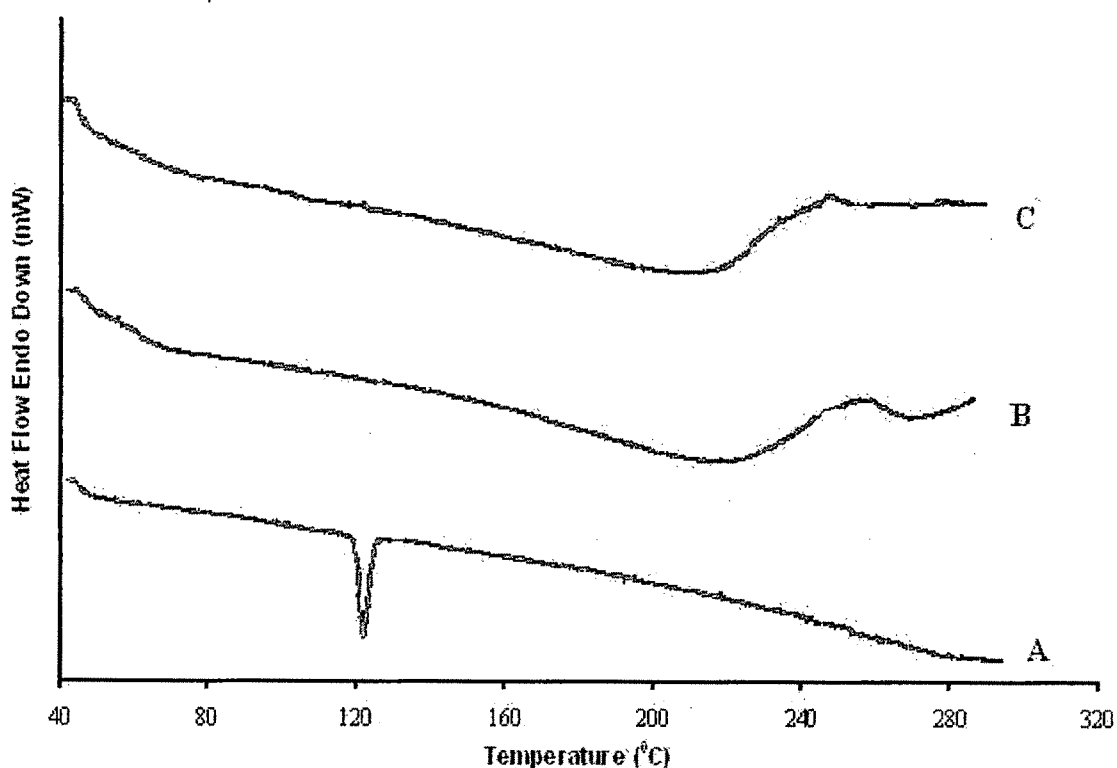
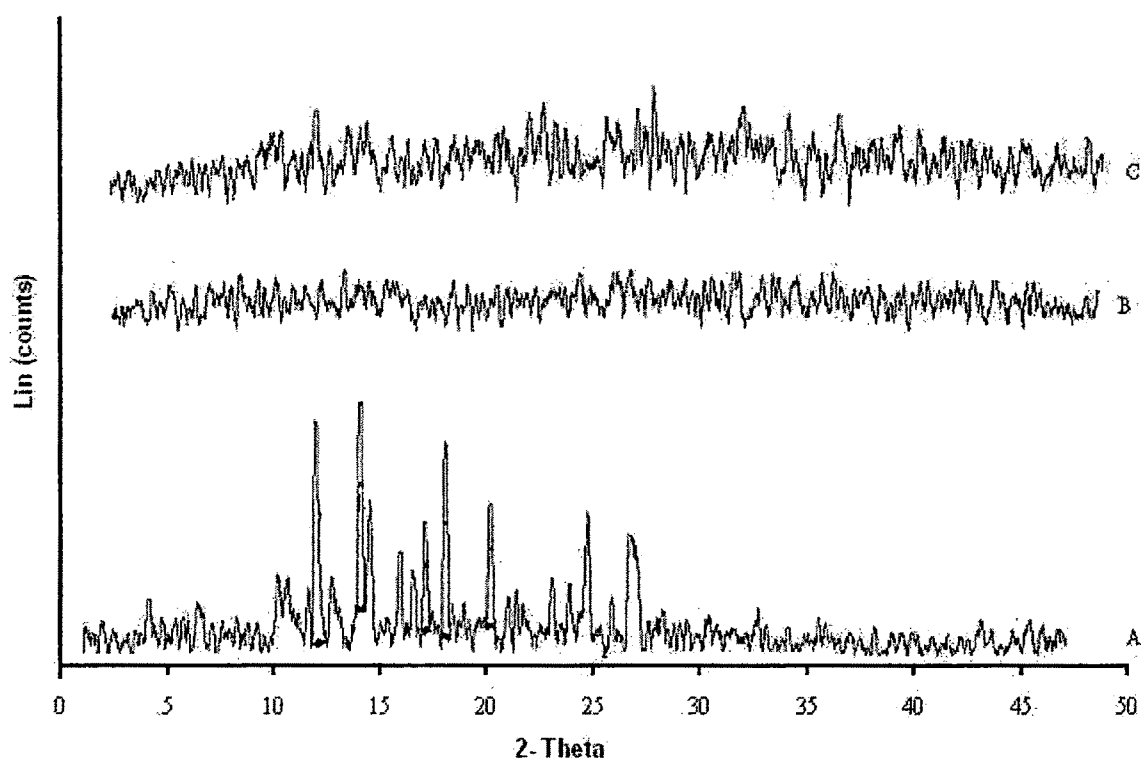


Fig. 5.4 DSC thermograms of (A) pure carvedilol; (B) placebo microspheres; (C) drug loaded microspheres.

### 5.8.7 X-ray diffraction (XRD) studies

XRD patterns recorded for plain carvedilol (A), placebo microspheres (B) and carvedilol loaded microspheres (C) are presented in Fig. 5.5. Carvedilol peaks observed at  $2\theta$  of  $11.18^\circ$ ,  $12.80^\circ$ ,  $13.48^\circ$ ,  $15.06^\circ$ ,  $17.38^\circ$ ,  $18.29^\circ$ ,  $20.15^\circ$ ,  $24.18^\circ$  and  $26.02^\circ$  are due to the crystalline nature of carvedilol. These peaks were not observed in the carvedilol loaded microspheres. This indicates that drug particles are dispersed at molecular level in the polymer matrices since no indication about the crystalline nature of the drugs was observed in the drug loaded microspheres.



**Fig. 5.5 Powder X-ray diffraction patterns of (A) pure carvedilol; (B) placebo microspheres; (C) drug loaded microspheres.**

### 5.8.8 In vitro drug release

The in vitro drug release profile of CRV from the alginate microspheres is shown in Fig. 5.6 and Fig. 5.7. The release pattern showed a moderate and controlled release following near zero order release. *In vitro* drug release proportionally increased with increasing the drug concentration. A slight decrease in the rate and extent of drug

## 5. Experimental - Carvedilol loaded Alginate Microspheres

release was observed with the increase in polymer amount in microspheres and is attributed to an increase in the density of the polymer matrix and to the diffusional path length that the drug molecules have to traverse. As expected (Thanoo et al., 1992), with an increase in the crosslinking agent concentration, a respective decrease in the rate and extent of drug release was observed. The cross-linking/ionotropic gelation of sodium alginate matrix with calcium chloride is well established. Sodium alginate is a linear copolymer consisting of  $\beta(1 \rightarrow 4)$  mannuronic acid (M) and  $\alpha(1 \rightarrow 4)$  L guluronic acid (G) residues. These uronic acid residues are arranged in homopolymeric block of type MM, GG, or heteropolymeric block of MG. The principle of cross-linking or gelation of sodium alginate with calcium chloride is based on the formation of tight junction between the GG residues.

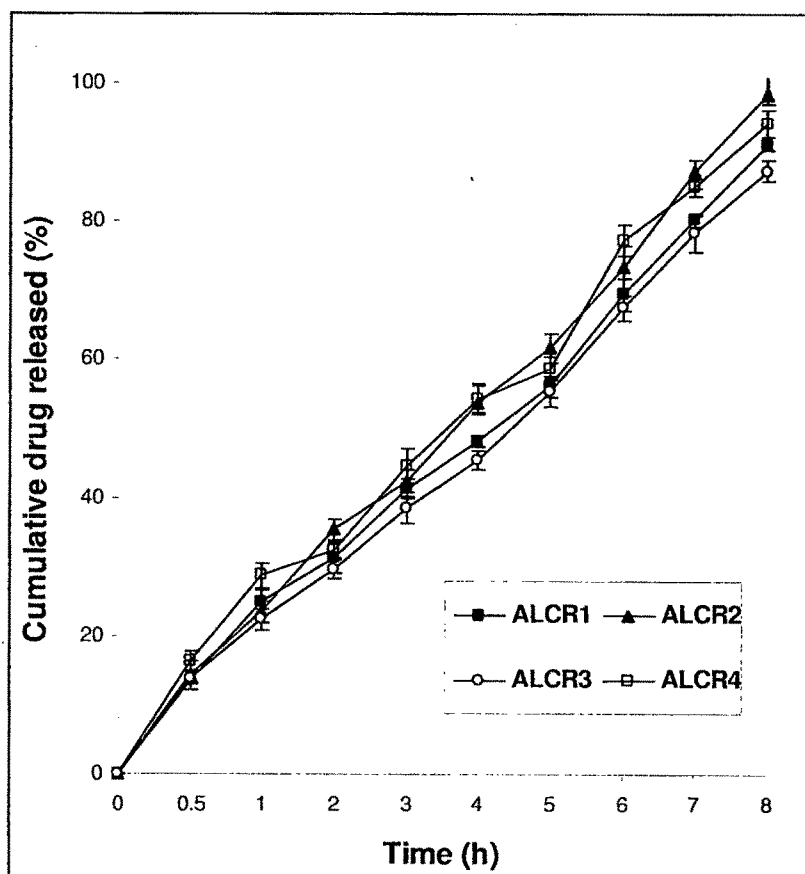


Fig. 5.6 *In vitro* drug release profile of alginate microspheres of CRV (Batches ALCR1 to ALCR4). The values are mean  $\pm$  SD ( $n = 3$ ).

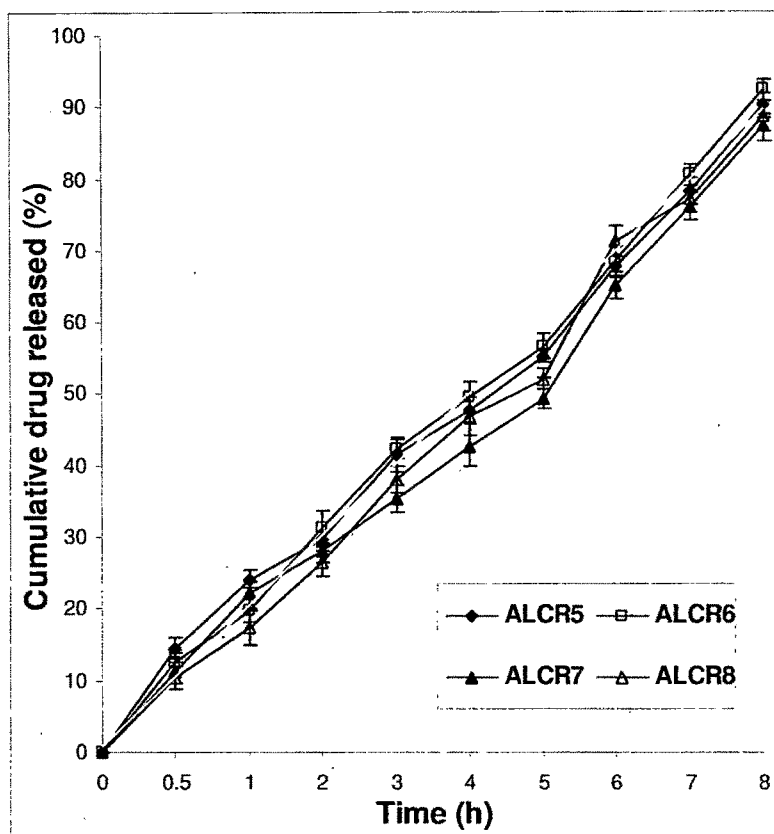


Fig. 5.7 *In vitro* drug release profile of alginate microspheres of CRV (Batches ALCR5 to ALCR8). The values are mean  $\pm$  SD ( $n = 3$ )

#### Mathematical modeling of release kinetics

In order to understand the mechanism and kinetics of drug release, the data was fitted to various kinetic equations. Three kinetic models including the zero-order release equation ( $Q_t = K_1 t$ ), first-order equation ( $Q_t = Q_0 e^{-K_2 t}$ ), and Higuchi equation ( $Q_t = K_3 t^{1/2}$ ) were applied to process the *in vitro* data to find the equation with the best fit (James et al., 1994; Wu et al., 1994; Jones et al, 2004; Costa et al, 2001). Where  $Q_t$  is the release percentage at time  $t$ .  $K_1$ ,  $K_2$ , and  $K_3$  are the rate constants of zero-order, first-order, and Higuchi respectively. The following plots were plotted:  $Q_t$  vs.  $t$  (zero order kinetic model);  $\log(Q_0 - Q_t)$  vs.  $t$  (first order kinetic model) and  $Q_t$  vs. square root of  $t$  (Higuchi model). Where  $Q_t$  is the amount of drug released at time  $t$  and  $Q_0$  is the initial amount of drug present in microspheres (Korsmeyer et al, 1983). The linear regression analyses are summarized in Table 5.4. A model with the greatest regression coefficient ( $r^2$ ) was chosen as the dominant model.

Table 5.4 Kinetic model of Carvedilol release from Alginate microspheres

Formulation code	Regression coefficient (r <sup>2</sup> )			Release kinetics
	Zero-order	First-order	Higuchi model	
ALCR1	0.9828	0.8774	0.9590	Zero-order
ALCR2	0.9871	0.7454	0.9663	Zero-order
ALCR3	0.9866	0.9144	0.9583	Zero-order
ALCR4	0.9754	0.8742	0.9583	Zero-order
ALCR5	0.9824	0.8718	0.9555	Zero-order
ALCR6	0.9887	0.8648	0.9700	Zero-order
ALCR7	0.9816	0.8834	0.9366	Zero-order
ALCR8	0.9911	0.9102	0.9628	Zero-order

In order to further investigate the release mechanism, the data were analyzed using the Peppas equation (Peppas, 1985; Ritger and Peppas, 1987),

$$\frac{M_t}{M_\infty} = kt^n \quad \dots\dots\dots 5.5$$

Here  $M_t$  is the amount of drug released at time  $t$ ,  $M_\infty$  is the amount released at time  $\infty$ ,  $M_t/M_\infty$  is the fraction of drug released at time  $t$ ,  $k$  is a constant characteristic of the drug-polymer system and  $n$  is the diffusional exponent, a measure of the primary mechanism of drug release. Using the least squares procedure, the values of  $n$ ,  $k$  and correlation coefficient ( $r^2$ ) were estimated (Table 5.5). In spherical matrices, if  $n \leq 0.43$ , a Fickian diffusion (case-I),  $0.43 \leq n < 0.85$ , anomalous or non-Fickian transport and  $n \geq 0.85$ , a case-II transport (zero order) drug release mechanism dominates. The values of  $n$  for all the batches ranged from 0.60 to 0.75 with correlation coefficient close to 0.99, indicating non-Fickian or anomalous type of transport (Mundargi et al., 2008).

Table 5.5 Release kinetics parameters and mechanisms of different formulations

Batch code	n	k	Correlation coefficient, $r^2$	Release mechanism
ALCR1	0.64	0.231	0.9805	Non-Fickian
ALCR2	0.66	0.221	0.9896	Non-Fickian
ALCR3	0.64	0.234	0.9857	Non-Fickian
ALCR4	0.60	0.258	0.9674	Non-Fickian
ALCR5	0.62	0.236	0.9788	Non-Fickian
ALCR6	0.70	0.202	0.9951	Non-Fickian
ALCR7	0.68	0.211	0.9681	Non-Fickian
ALCR8	0.75	0.179	0.9909	Non-Fickian

## 5.9 Optimization data analysis and model-validation

### 5.9.1 Fitting of data to the model

The three factors with lower and upper design points in coded and uncoded values are shown in Table 5.1. The ranges of responses Y1 and Y2 were 26.36–54.32  $\mu\text{m}$  and 69.25–85.28% respectively. All the responses observed for eight formulations prepared were fitted to various models using Design- Expert<sup>®</sup> software. It was observed that the best-fitted models were linear and interactive. The values of  $R^2$ , adjusted  $R^2$ , predicted  $R^2$ , SD and % CV are given in Table 5.6 along with the regression equation generated for each response. The results of ANOVA in Table 5.7 for the dependent variables demonstrate that the model was significant for both the response variables.

**5. Experimental - Carvedilol loaded Alginate Microspheres**

**Table 5.6 Summary of results of regression analysis for responses Y1 and Y2**

Models	Adjusted		Predicted	SD	% CV	P
	R <sup>2</sup>	R <sup>2</sup>	R <sup>2</sup>			
<b>Response (Y1)</b>						
Linear model	0.9506	0.9135	0.8023	2.860	6.93	0.0045
<b>Response (Y2)</b>						
<b>Interactive</b>						
model	1.0000	0.9997	0.9970	0.095	0.12	0.0129
Regression equations of the fitted linear and interactive model						
Y1 = 41.18 + 8.10X <sub>1</sub> + 1.32X <sub>2</sub> + 3.32X <sub>3</sub>						
Y2 = 76.60 - 3.50X <sub>1</sub> - 1.48X <sub>2</sub> - 3.00X <sub>3</sub> + 0.38 X <sub>1</sub> X <sub>2</sub> + 0.66X <sub>1</sub> X <sub>3</sub> - 0.38X <sub>2</sub> X <sub>3</sub>						

**Table 5.7 Results of analysis of variance for measured response**

Parameters	DF*	SS*	MS*	F*	Significance F
<b>Particle size</b>					
Model	3	627.31	209.1	25.65	0.0045 significant
Residual	4	32.61	8.15	---	---
Total	7	659.92	---	---	---
<b>In vitro mucoadhesion</b>					
Model	6	193.48	32.25	3538.7	0.0129 significant
Residual	1	9.11E-03	9.11E-03	---	---
Total	7	193.49	---	---	---

\*DF indicates degrees of freedom; SS sum of square; MS mean sum of square and F is Fischer's ratio.

It was observed that all the three independent variables viz.  $X_1$  (drug: polymer weight ratio),  $X_2$  (concentration of  $\text{CaCl}_2$ ) and  $X_3$  (cross linking time) had positive effect on particle size (Y1), but, negative effect on *in vitro* mucoadhesion (Y2). The effect of drug : polymer weight ratio on the particle size of the microspheres was twice greater than the cross linking time and six fold more than  $\text{CaCl}_2$  concentration. The coefficients with more than one factor term in the regression equation represent interaction terms. It also shows that the relationship between factors and responses is not always linear. When more than one factors are changed simultaneously and used at different levels in a formulation, a factor can produce different degrees of response. The interaction effect of  $X_1$  and  $X_2$ ;  $X_1$  and  $X_3$  was favorable (positive), whereas interaction effect of  $X_2$  and  $X_3$  was unfavorable (negative) for response Y2. From these equations (Table 5.6), it is quite clear that the drug : polymer weight ratio plays an important role on *in vitro* mucoadhesion of the microspheres.

### **5.9.2 Contour plots and response surface analysis**

Three dimensional response surface plots generated by the Design Expert<sup>®</sup> software are presented in Fig. 5.8-5.10 and Fig. 5.14-5.16 while two dimensional contour plots are presented in Fig. 5.11-5.13 and Fig. 5.17-5.19 for the studied responses i.e. particle size and *in vitro* mucoadhesion. In all the presented figures, the third factor was kept at a constant level. Fig. 5.8 and Figure 5.11 depicts response surface, contour plots of the effects of drug: polymer ratio ( $X_1$ ) and  $\text{CaCl}_2$  concentration ( $X_2$ ) on particle size which indicate a linear effect on particle size of the microspheres. The combined effects of  $\text{CaCl}_2$  concentration ( $X_2$ ) and cross linking time ( $X_3$ ) and drug: polymer ratio ( $X_1$ ) and cross linking time ( $X_3$ ) on particle size as shown in Fig. 5.9, 5.10 and Fig. 5.12, 5.13 are also linear. This explains that higher the amount of  $\text{CaCl}_2$  or higher the time of cross linking, more will be the cross-linking of the guluronic acid units of sodium leading to formation of larger microspheres.

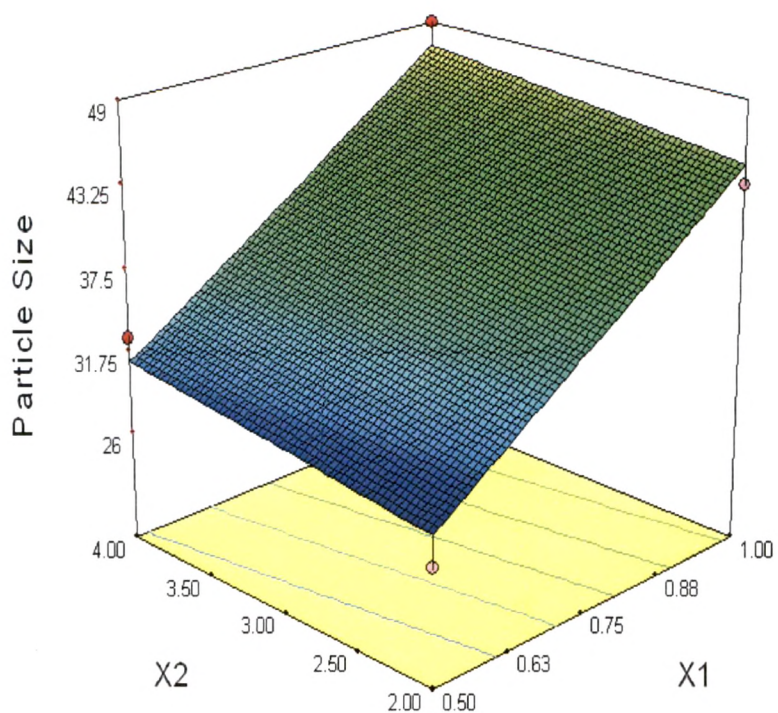


Fig. 5.8 Response surface plots for the (a) effects of drug: polymer ratio (X1) and  $\text{CaCl}_2$  concentration (X2) on particle size (Y1).

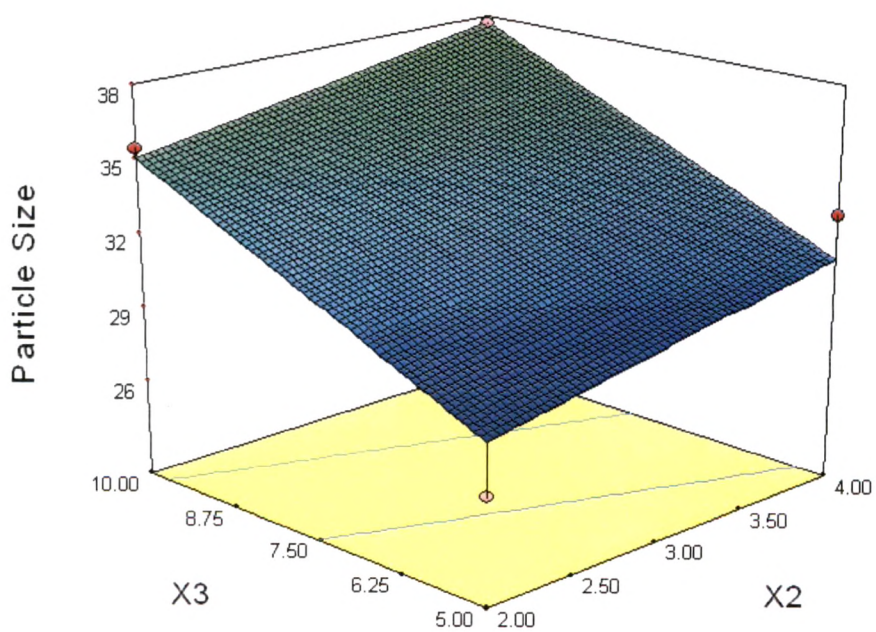


Fig. 5.9 Response surface plots for the effects of  $\text{CaCl}_2$  concentration (X2) and cross linking time (X3) on particle size (Y1).

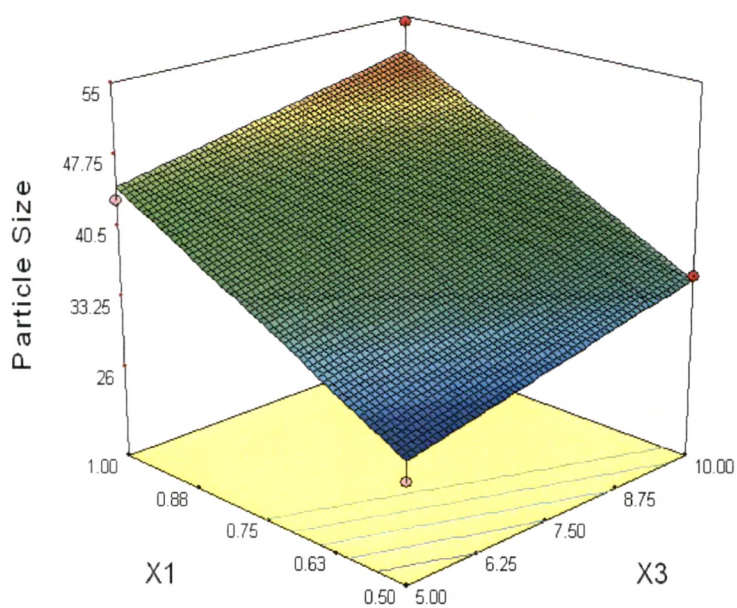


Fig. 5.10 Response surface plots for the effects of drug: polymer ratio (X1) and cross linking time (X3) on particle size (Y1).

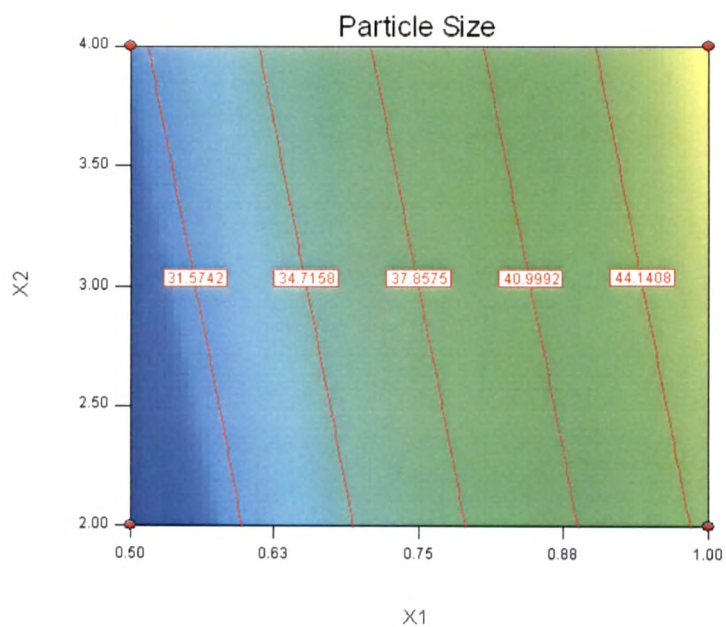


Fig. 5.11 Contour plots for the effects of drug: polymer ratio (X1) and  $\text{CaCl}_2$  concentration (X2) on particle size (Y1).

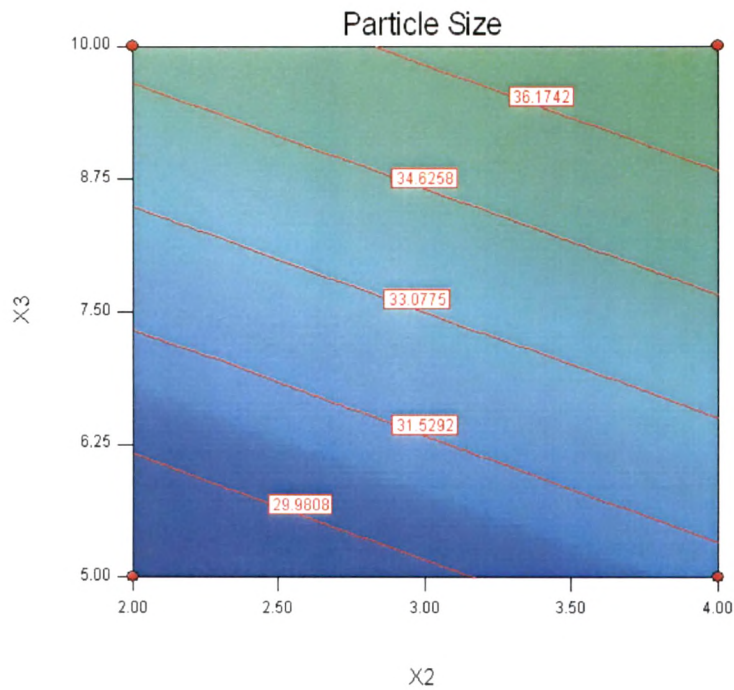


Fig. 5.12 Contour plots for the effects of CaCl<sub>2</sub> concentration (X<sub>2</sub>) and cross linking time (X<sub>3</sub>) on particle size (Y<sub>1</sub>).

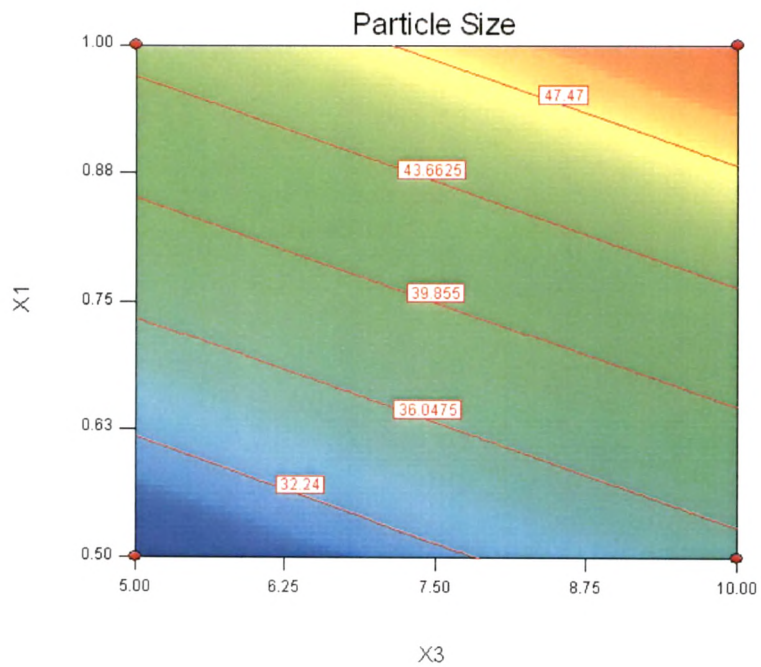


Fig. 5.13 Contour plots for the effects of drug: polymer ratio (X<sub>1</sub>) and cross linking time (X<sub>3</sub>) on particle size (Y<sub>1</sub>).

The combined effect of  $X_1$  and  $X_2$  on in vitro mucoadhesion of the microspheres was observed to be non linear as in Fig. 5.14 and 5.17. At low value of drug: polymer ratio and  $\text{CaCl}_2$  concentration, higher value for in vitro mucoadhesion was observed. Similar effects were observed for factors  $X_2$ ,  $X_3$  and  $X_1$ ,  $X_3$  as shown in Fig. 5.15, 5.16 and Fig. 5.18, 5.19 respectively. As the  $\text{CaCl}_2$  concentration and cross linking time increased from low to high, the value for in vitro mucoadhesion of the microspheres was decreased.

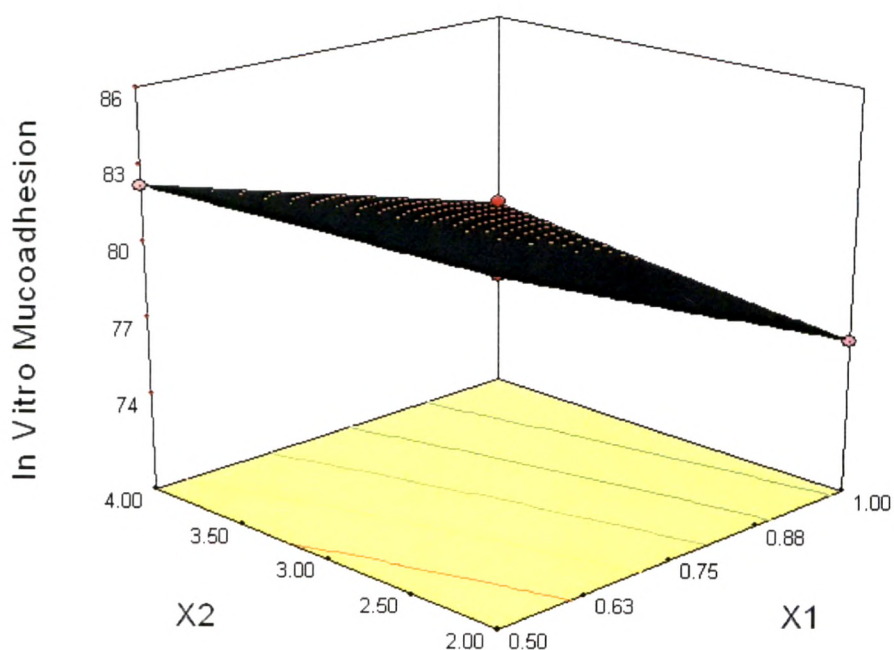


Fig. 5.14 Response surface plots for the effects of drug: polymer ratio ( $X_1$ ) and  $\text{CaCl}_2$  concentration ( $X_2$ ) on in vitro mucoadhesion ( $Y_2$ ).

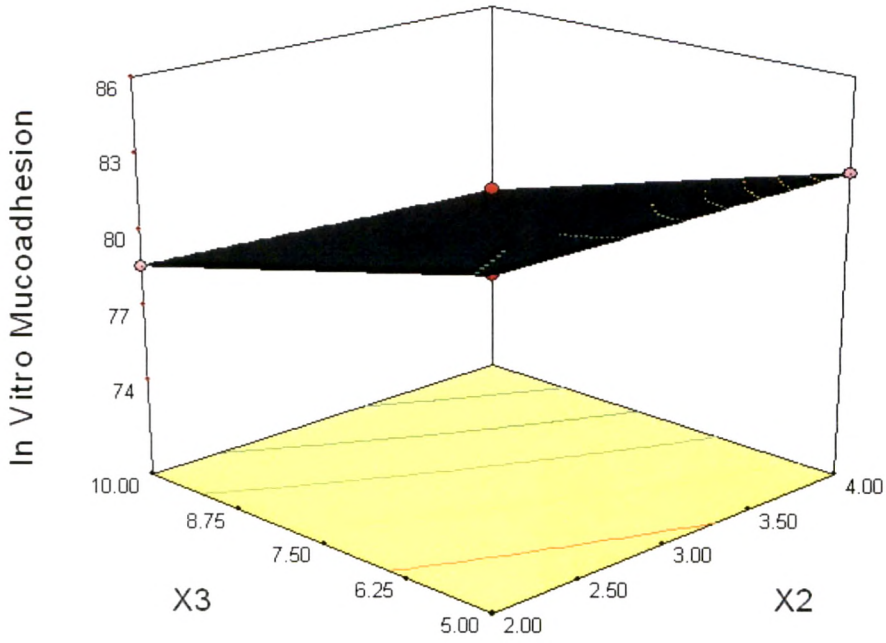


Fig. 5.15 Response surface plots for the effects of CaCl<sub>2</sub> concentration (X2) and cross linking time (X3) on in vitro mucoadhesion (Y2).

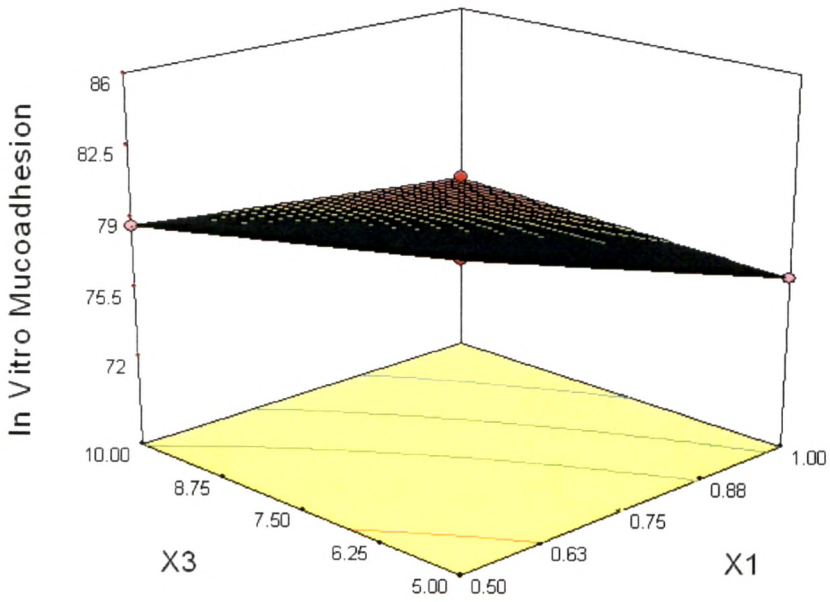


Fig. 5.16 Response surface plots for the effects of drug: polymer ratio (X1) and cross linking time (X3) on in vitro mucoadhesion (Y2).

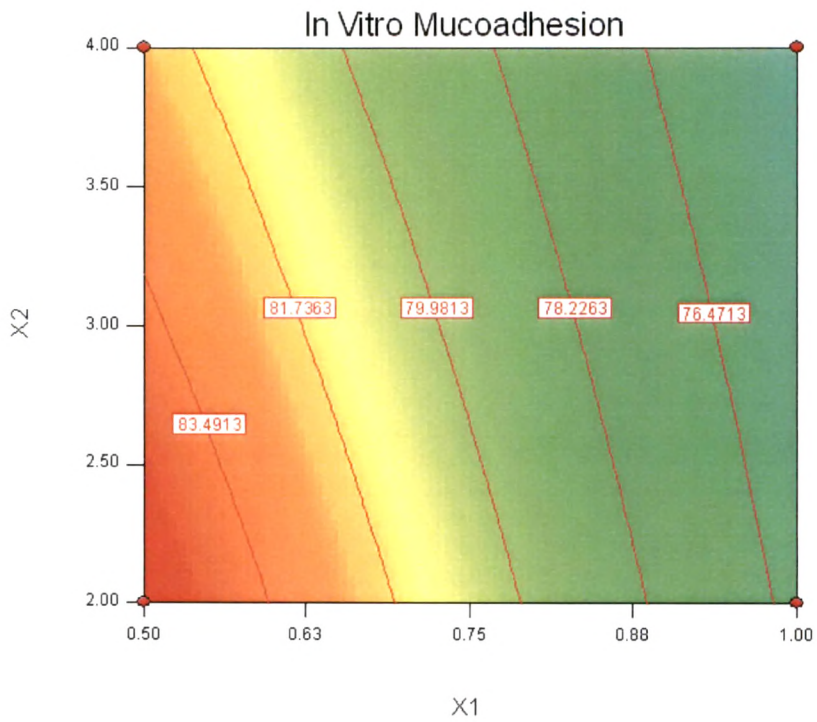


Fig. 5.17 Contour plots for the effects of drug: polymer ratio (X1) and  $\text{CaCl}_2$  concentration (X2) on in vitro mucoadhesion (Y2).

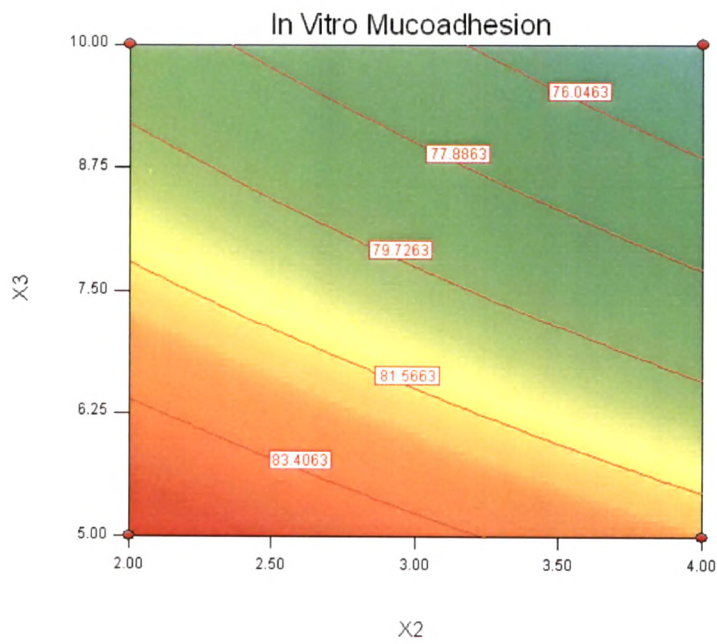
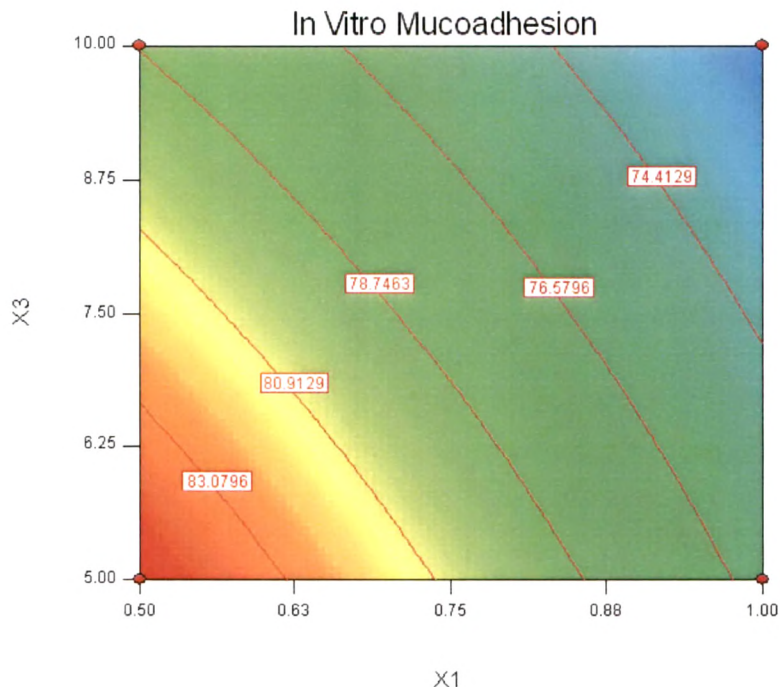


Fig. 5.18 Contour plots for the effects of  $\text{CaCl}_2$  concentration (X2) and cross linking time (X3) on in vitro mucoadhesion (Y2).



**Fig. 5.19** Contour plots for the effects of drug: polymer ratio (X1) and cross linking time (X3) on in vitro mucoadhesion (Y2).

### 5.9.3 Optimization and validation

A numerical optimization technique by the desirability approach was used to generate the optimum settings for the formulation. The process was optimized for the dependent (response) variables Y1 and Y2. The optimum formulation was selected based on the criteria of attaining the minimum value of particle size and maximum value of in vitro mucoadhesion. Formulation F1 having drug: polymer ratio (1:2), CaCl<sub>2</sub> concentration (2%) and cross linking time (5 min) fulfilled all the criteria set from desirability search. To gainsay the reliability of the response surface model, new optimized formulation (as per formula ALCR1) was prepared according to the predicted model and evaluated for the responses.

The result in Table 5.8 illustrates the comparison between the observed and predicted values of both the responses Y1 and Y2 for all the formulations is presented. It can be seen that in all cases there was a reasonable agreement between the predicted and the experimental values as prediction error was found to vary between -7.28% and +5.94%. For this reason it can be concluded that the equations describe adequately the

### 5. Experimental - Carvedilol loaded Alginate Microspheres

influence of the selected independent variables on the responses under study. This indicates that the optimization technique was appropriate for optimizing the alginate microsphere formulation. The linear correlation plots drawn between the predicted and experimental values for all the batches of the microspheres are shown in Fig. 5.20 and Fig. 5.21 which demonstrated high values of  $R^2$  (0.9506 and 0.9996). Thus the low magnitudes of error as well as the significant values of  $R^2$  in the present investigation prove the high prognostic ability of the optimization technique by factorial design.

**Table 5.8 The predicted and observed response variables of the sodium alginate microspheres.**

Responses	Formulation code	Predicted value	Observed value	Prediction error* (%)
Y1	ALCR1	28.43	26.36	-7.28
	ALCR2	44.63	43.28	-3.02
	ALCR3	31.08	32.85	5.69
	ALCR4	47.28	48.94	3.51
	ALCR5	35.07	35.46	1.11
	ALCR6	51.27	54.32	5.94
	ALCR7	37.72	37.64	-0.21
	ALCR8	53.92	50.58	-5.58
Y2	ALCR1	85.24	85.28	0.046
	ALCR2	76.41	76.12	-0.037
	ALCR3	82.29	82.26	-0.036
	ALCR4	74.71	74.75	0.053
	ALCR5	78.68	78.65	-0.038
	ALCR6	72.24	72.28	0.055
	ALCR7	74.2	74.24	0.053
	ALCR8	69.28	69.25	-0.043

\*Prediction error (%) = (Observed value – Predicted value)/ Predicted value x100%  
Y1 and Y2 are particle size and in vitro mucoadhesion respectively.

5. Experimental - Carvedilol loaded Alginate Microspheres

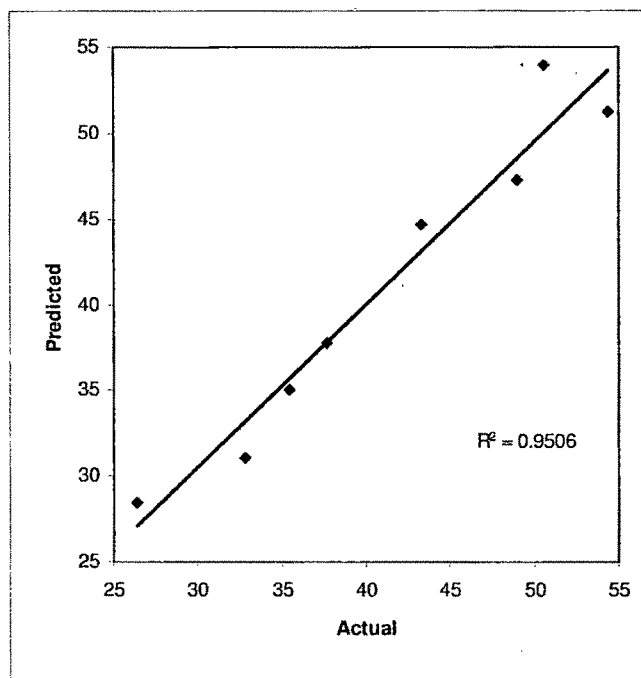


Fig. 5.20 Correlation between actual and predicted values for particle size

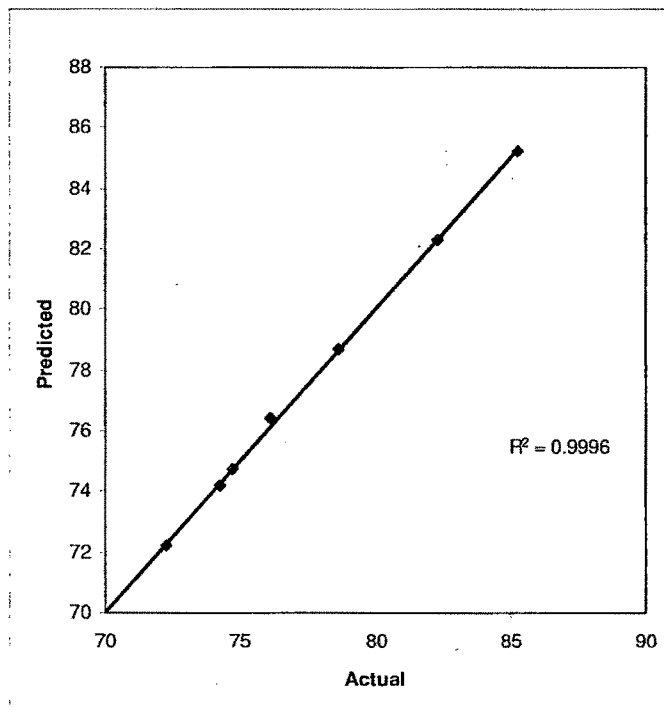


Fig. 5.21 Correlation between actual and predicted values for in vitro mucoadhesion

### **5.10 Histology studies**

The morphologic changes in the nasal mucosa caused by drugs, enhancers, or other formulation additives, may result in damage to the ability of the nasal mucosa to carry out its normal defence functions. In addition, chronic infection may occur when recovery or regeneration of the normal epithelium can not be achieved (Boling, 1935). Thus, it is important to study the histology of the nasal mucosa with the formulation. The histology of control and treated nasal mucosa after 8 h is shown in Fig. 5.22. The microscopic observations indicated that the optimized formulation has no significant effect on the microscopic structure of sheep nasal mucosa. The surface epithelium lining and the granular cellular structure of the nasal mucosa were totally intact. No major changes in the ultrastructure of mucosa morphology could be seen and the epithelial cells appeared mostly unchanged. Neither cell necrosis nor removal of the epithelium from the nasal mucosa was observed after diffusion study as compared with control mucosa treated with phosphate buffer pH 6.2. Thus, the microsphere formulation seems to be safe with respect to nasal administration.

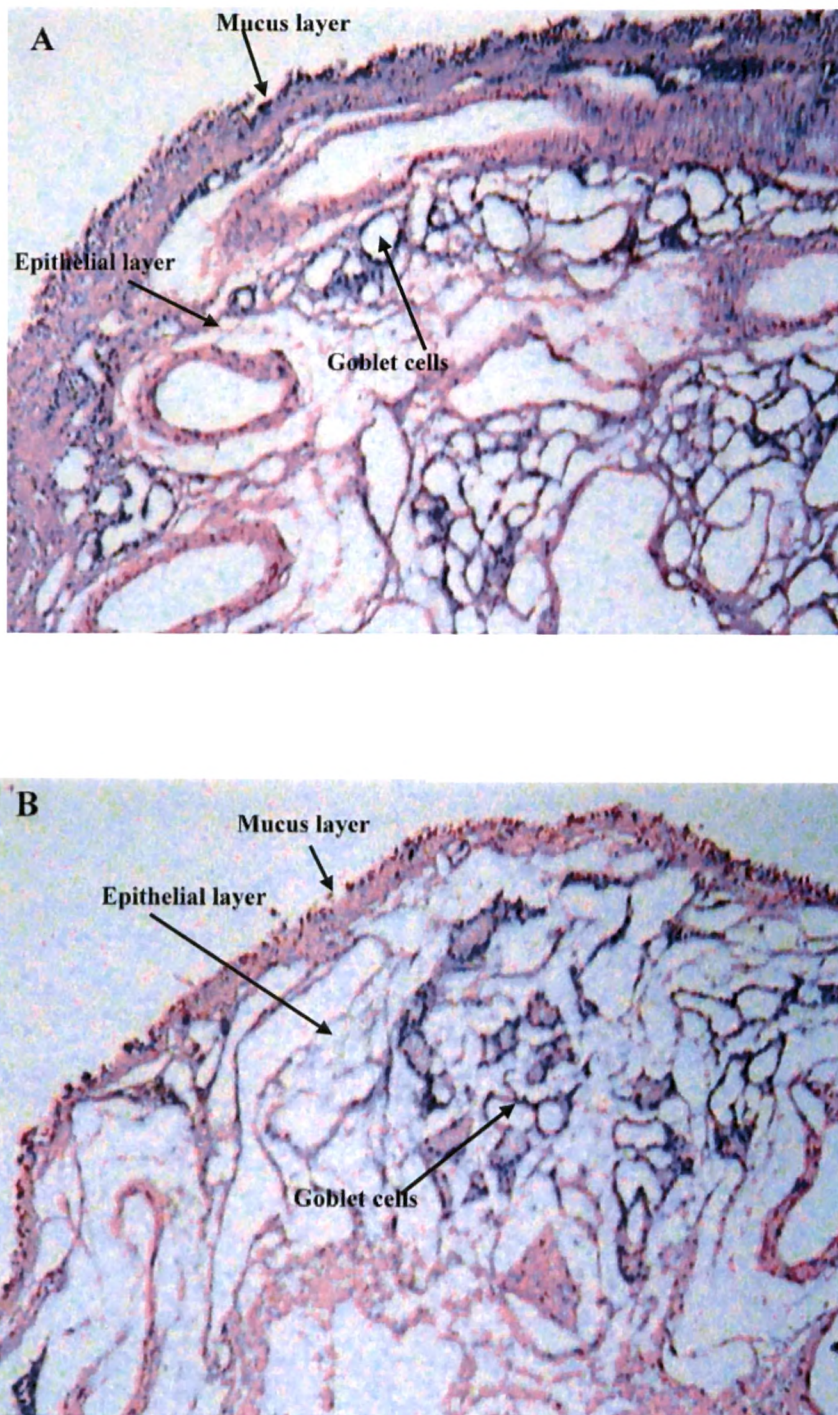


Fig. 5.22 Histology evaluations of sections of sheep nasal mucosa. (A) Control mucosa after incubation with phosphate buffer pH 6.2 in diffusion chamber; (B) Mucosa after incubation in diffusion chamber with microsphere formulation.

### 5.11 Stability studies

In view of potential utility of CRV loaded alginate microsphere formulation for nasal administration, the stability study was performed at 40°C/75% RH for 3 months (climatic zone IV conditions for accelerating testing). The stability data of the CRV loaded alginate microsphere formulation is shown in Table 5.9. No physical changes in the formulation were observed during storage. The results obtained in the stability test showed that the particle size and drug content of the formulations stored at 40°C/75% RH was unchanged during the 3-month period. Particle size and drug content values after 1, 2 and 3 months showed no significant differences ( $p>0.05$ ). This indicated that the alginate microsphere formulation of CRV was stable and could be stored at ambient conditions.

**Table 5.9 Stability study results for CRV loaded Alginate microspheres under accelerated condition**

Time/months	Appearance	Particle size* ( $\mu\text{m}$ )	Drug content* (%)
0	White	26.36 $\pm$ 1.24	100.0 $\pm$ 1.74
1	White	25.42 $\pm$ 2.88	99.85 $\pm$ 2.34
2	White	25.69 $\pm$ 3.12	98.38 $\pm$ 2.87
3	White	24.86 $\pm$ 2.46	98.06 $\pm$ 2.25

\*n = 3; Mean  $\pm$  SD

## REFERENCES

- Bhardwaj, S. B.; Shukla, A.J.; Collins, C. C.** Effect of varying drug loading on particle size distribution and drug release kinetics of verapamil hydrochloride microspheres prepared with cellulose esters. *J. Microencapsul.* **1995**, 12(1), 71-81.
- Boling, L. R.** Regeneration of nasal mucosa. *Arch. Otolaryng.* **1935**, 22, 689-742.
- Costa, P.; Sousa Lobo, J. M.** Modeling and comparison of dissolution profiles. *Eur. J. Pharm. Sci.* **2001**, 13, 123-33.
- Dhiman, M. K.; Yedurkar, P. D.; Sawant, K. K.** Buccal bioadhesive delivery system of 5-fluorouracil: optimization and characterization. *Drug Dev. Ind. Pharm.* **2008**, 34(7), 761-770.
- Dubernet, C.** Thermo analysis of microspheres. *Thermochim. Acta.* **1995**, 248, 259-269.
- Huang, Y. B.; Tsai, Y. H.; Lee, S. H.; Chang, J. S.; Wu P. C.** Optimization of pH-independent release of nicardipine hydrochloride extended-release matrix tablets using response surface methodology. *Int. J. Pharm.* **2005**, 289(1-2), 87-95.
- Illum, L.; Jorgensen, H.; Bisgaard, H.; Krosgaard, O.; Rossing, N.** Bioadhesive microspheres as a potential nasal drug delivery system. *Int. J. Pharm.* **1987**, 39, 189-199.
- Jones, D. S.; Lawlor, M. S.; Woolfson, A. D.** Formulation and characterisation of tetracycline-containing bioadhesive polymer networks designed for the treatment of periodontal disease. *Current Drug Del.* **2004**, 1, 17-25.
- Kincl, M.; Turk, S.; Vrečer, F.** Application of experimental design methodology in development and optimization of drug release method. *Int. J. Pharm.* **2005**, 291, 39-49.
- Korsmeyer, R. W.; Gurny, R.; Doelker, E.; Buri, P.; Peppas N. A.** Mechanisms of solute release from porous hydrophilic polymers. *Int. J. Pharm.* **1983**, 15, 25-35.

**Martnez-Sancho, C.;** Herrero-Vanrell, R.; Negro, S. Optimization of aciclovir poly (d,l-lactide-co-glycolide) microspheres for intravitreal administration using a factorial design study. *Int. J. Pharm.* **2004**, 273, 45-56.

**Mehta, A. K.;** Yadav, K. S.; Sawant, K. K. Nimodipine loaded PLGA nanoparticles: formulation optimization using factorial design, characterization and in vitro evaluation. *Current Drug Del.* **2007**, 4(3), 185-93.

**Mu, L.;** Feng, S. S. Fabrication characterization and in vitro release of paclitaxel (Taxol) loaded poly (lactic-co-glycolic acid) microspheres prepared by spray drying technique with lipid/cholesterol emulsifiers. *J. Control. Release* **2001**, 76, 239-254.

**Narendra, C.;** Srinath, M. S.; Prakash Rao, B. Development of three layered buccal compact containing metoprolol tartrate by statistical optimization technique. *Int. J. Pharm.* **2005**, 304(1-2), 102-114.

**Peppas, N. A.** Analysis of Fickian and non-Fickian drug release from polymers. *Pharm. Acta Helv.* **1985**, 60, 110-11.

**Peppas, N. A.;** Buri, P. A. Surface, interfacial and molecular aspects of polymer bioadhesion on soft tissues. *J. Control. Rel.* **1985**, 2, 257-275.

**Ritger, P. L.;** Peppas, N. A. A simple equation for description of solute release II. Fickian and anomalous release from swellable devices. *J. Control. Rel.* **1987**, 5, 37-42.

**Singh, B.;** Ahuja, N. Development of controlled-release buccoadhesive hydrophilic matrices of diltiazem hydrochloride: optimization of bioadhesion, dissolution, and diffusion parameters. *Drug Dev. Ind. Pharm.* **2002**, 28(4), 431-442.

**Vandervoort, J.;** Ludwig, A. Preparation factors affecting the properties of polylactide nanoparticles: a factorial design study. *Pharmazie* **2001**, 56, 484-488.

**Wan, L. S.C.;** Heng, P. W. S.; Chan, L. W. Drug encapsulation in alginate microspheres by emulsification. *J. Microencapsul.* **1992**, 9(3), 309-316.